Electronic Supplementary Material (ESI) for Analytical Methods.

Naphthalimide-tyrosine-based dicationic amphiphile for intracellular '*turn-on*' simultaneous detection of ATP and CTP

Poonam Sharma[a], Sugandha Kumar[b], Amandeep Walia[c], Satwinder Singh Marok[d], Vanita Vanita*[c] and Prabhpreet Singh*[a]

[a]*Department of Chemistry, UGC Centre for Advanced Studies-II, Guru Nanak Dev University, Amritsar 143001 (Pb.)-India*

[b]*School of Physical Sciences, Starex University, Gurugram*

[c]*Department of Human Genetics, Guru Nanak Dev University, Amritsar (Pb.)-India*

[d]*Apotex Inc.,150 Signet Drive, Toronto, ON, M9L1T9 Canada*

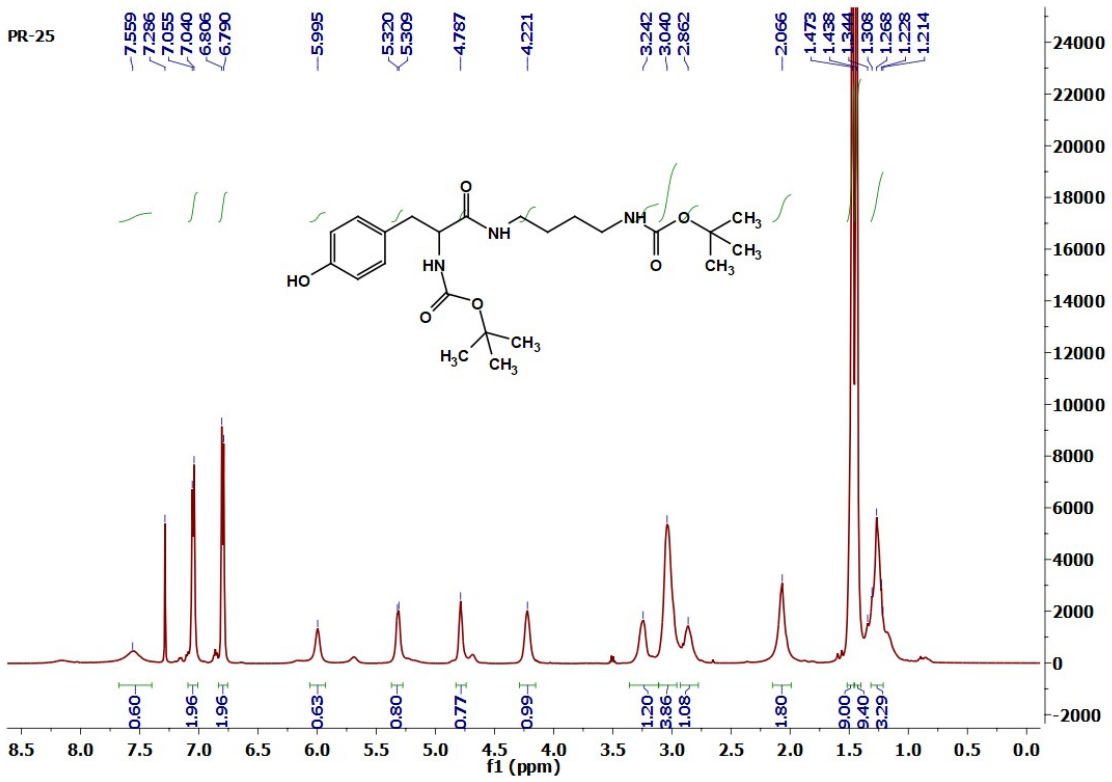

Figure 1a: ^{1}H NMR Spectrum of compound **2**.

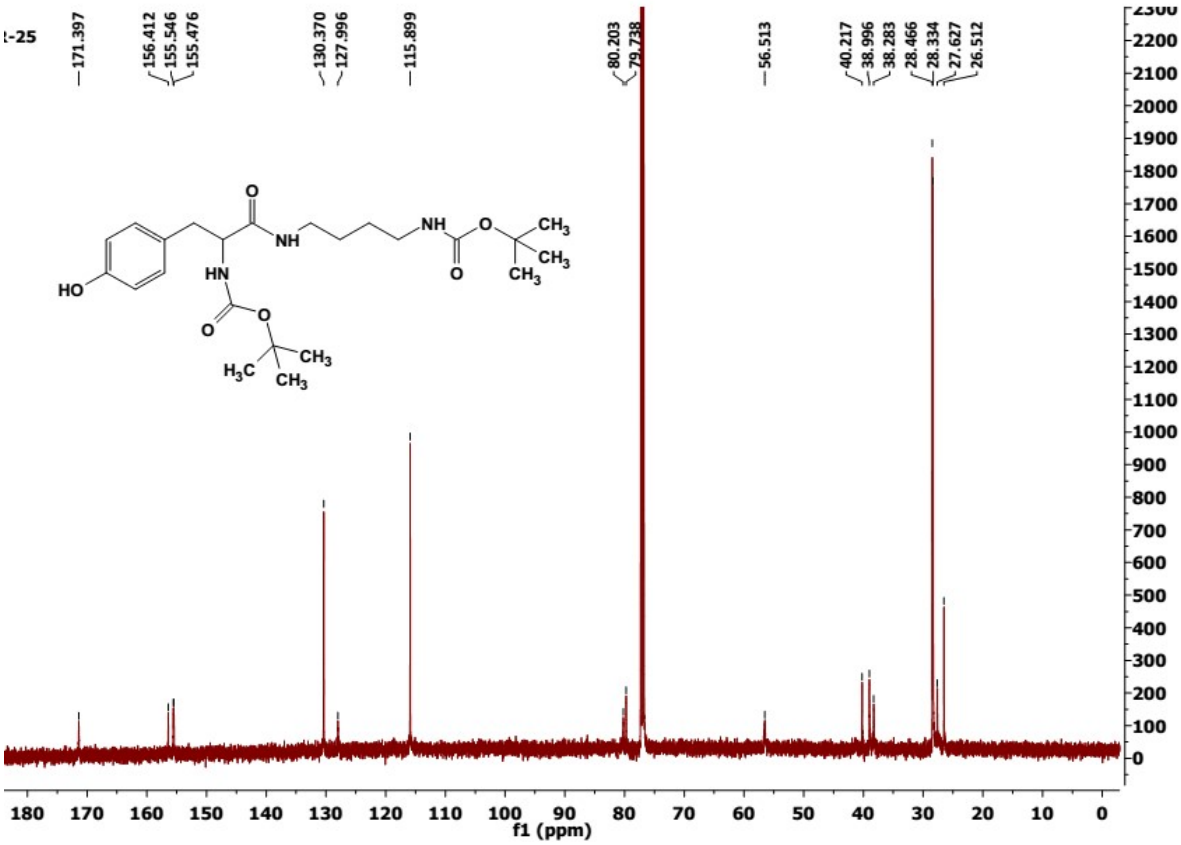

Figure 1b: ^{13}C NMR Spectrum of compound **2**.

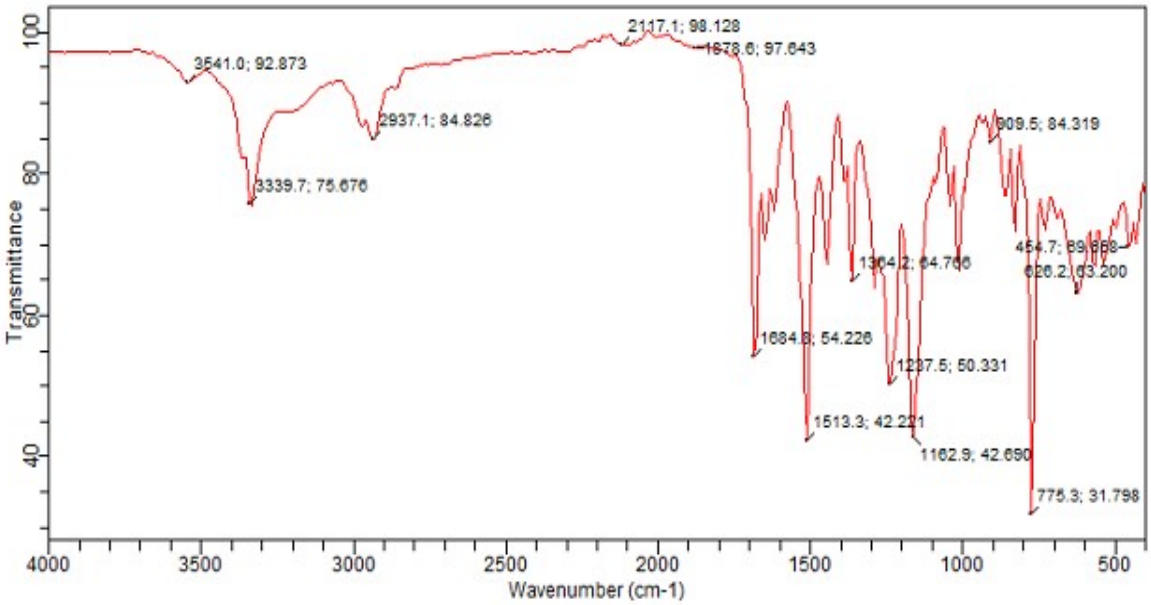

Figure 1c: FTIR Spectrum of compound **2**.

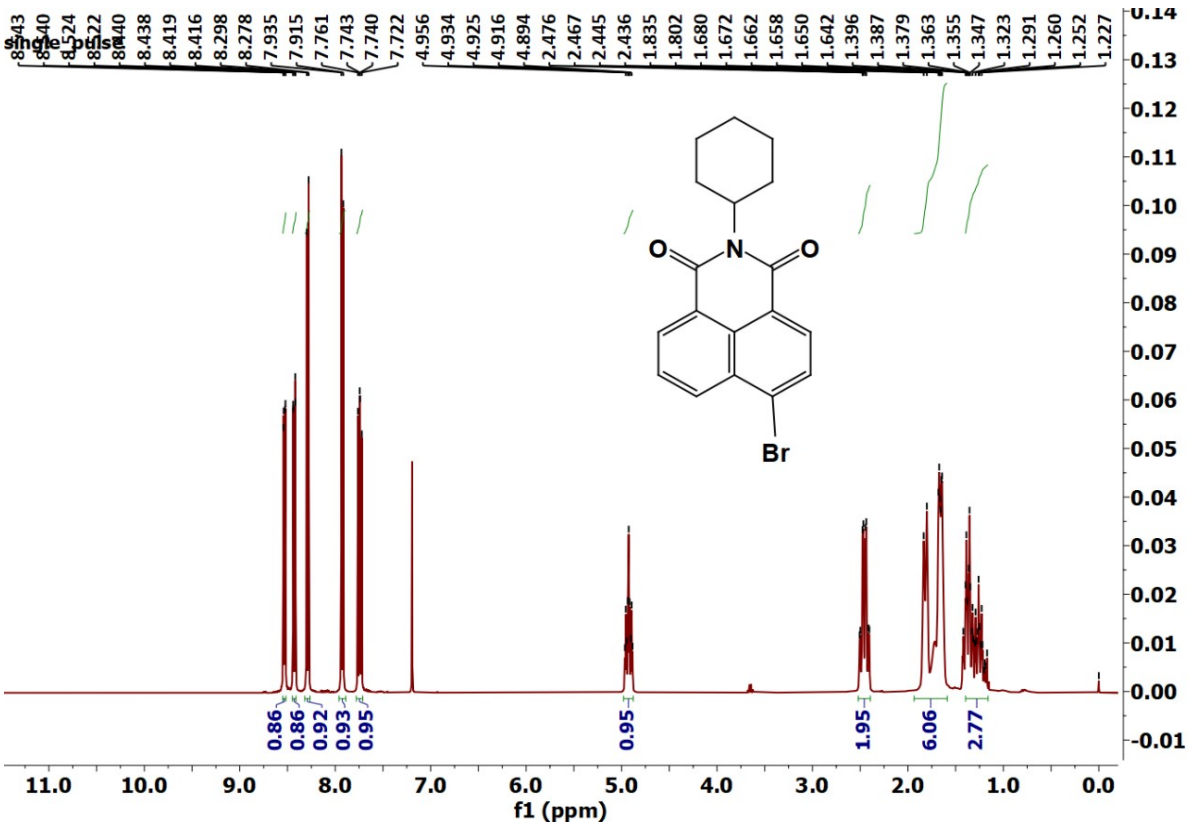

Figure 2a: ^{1}H NMR Spectrum of compound **3**.

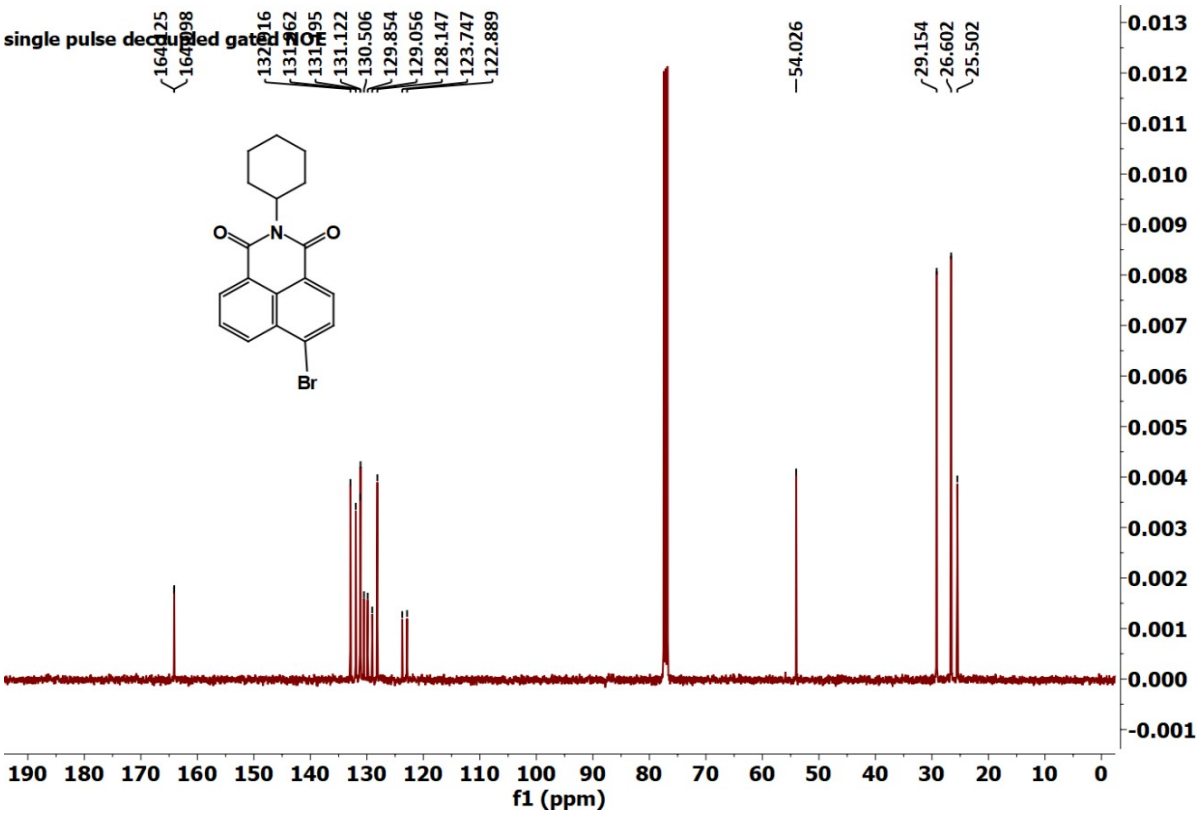

Figure 2b: ^{13}C NMR Spectrum of compound **3**.

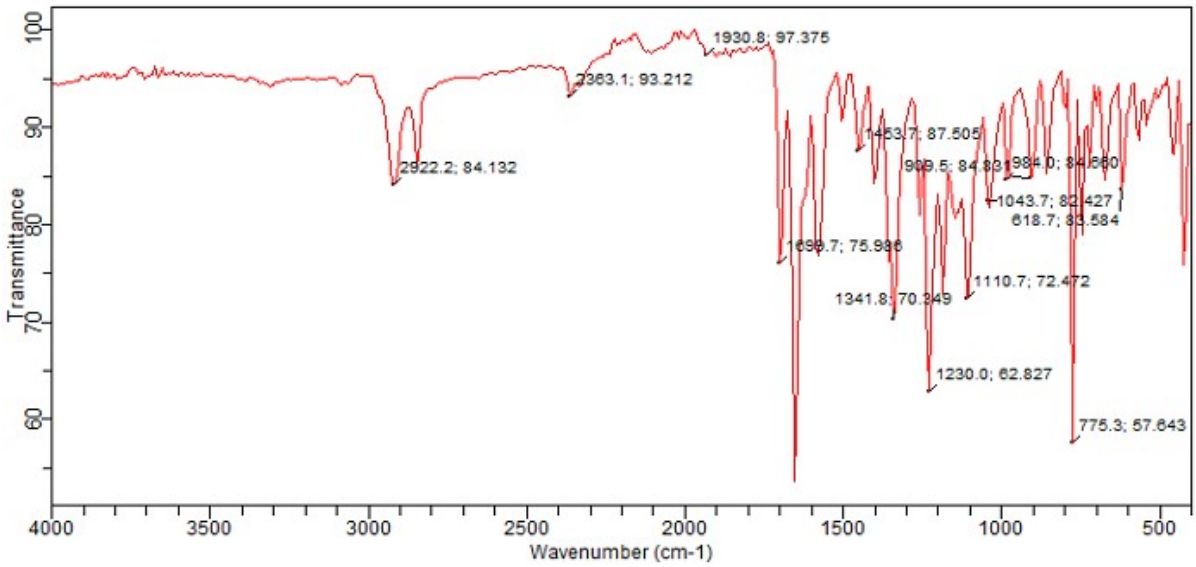

Figure 2c: FTIR Spectrum of compound **3**.

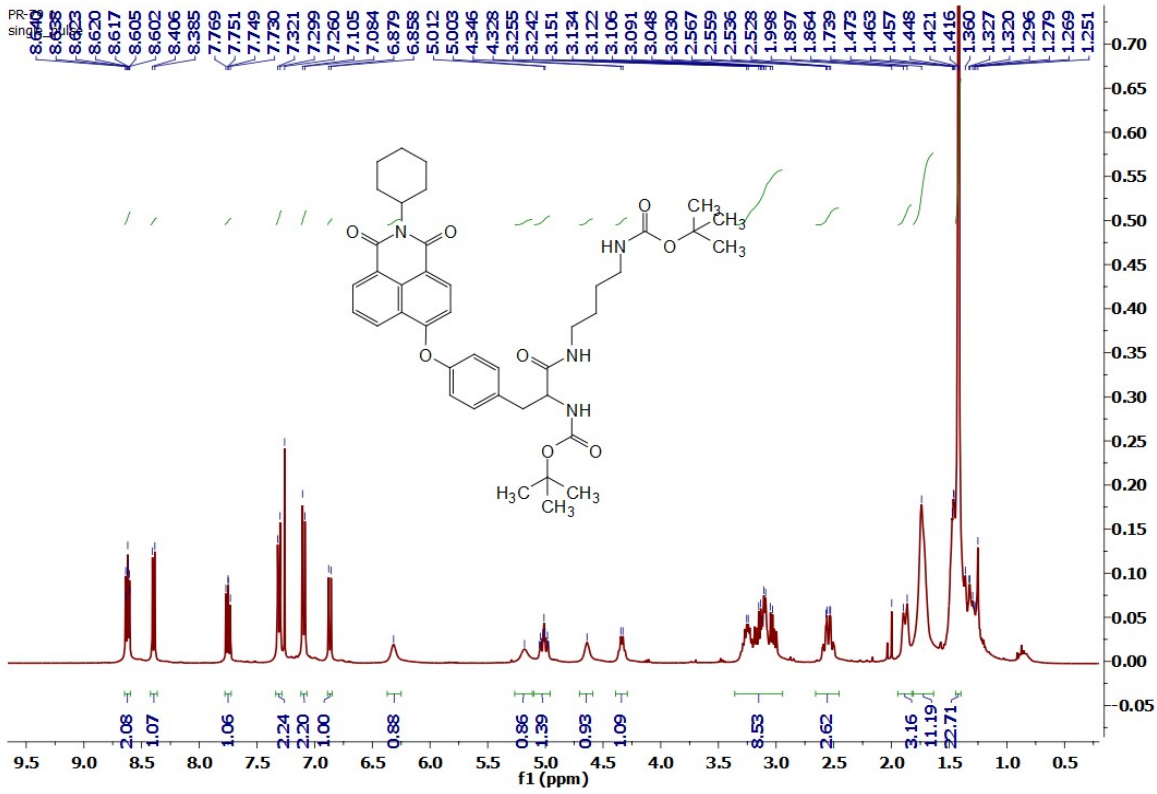

Figure 3a: ^{1}H NMR Spectrum of compound **4.**

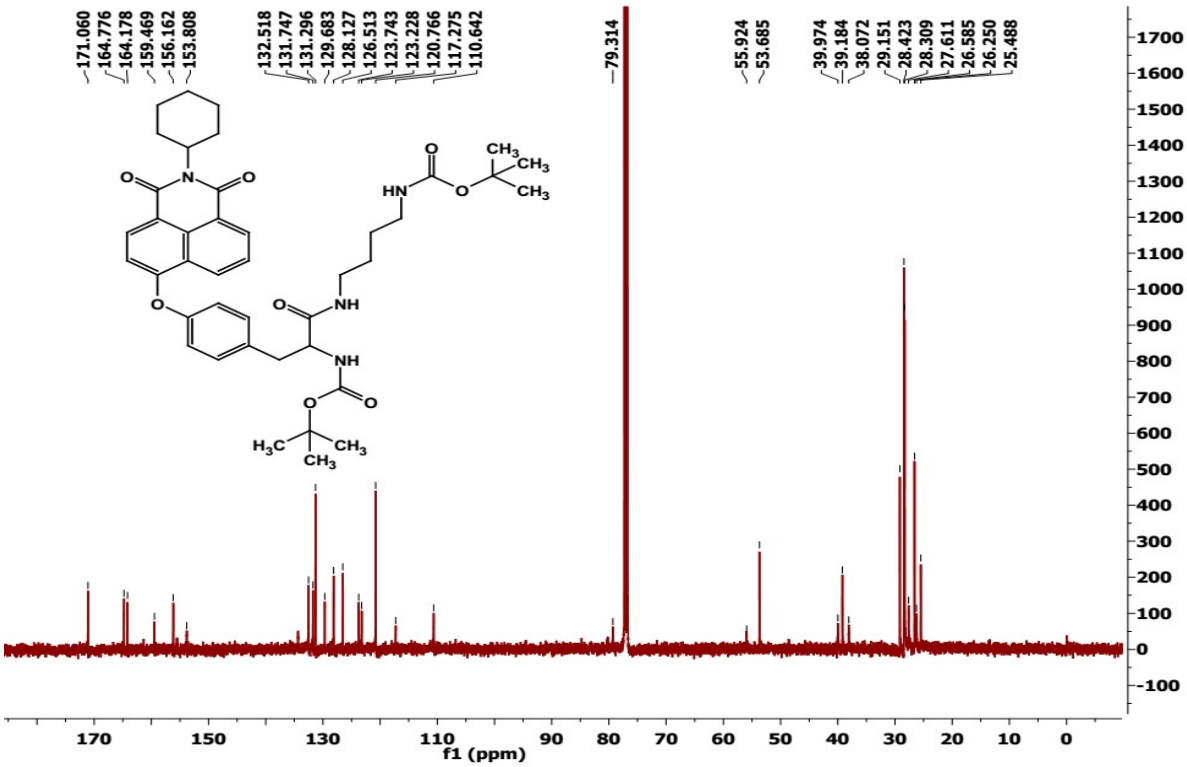

Figure 3b: ^{13}C NMR Spectrum of compound **4.**

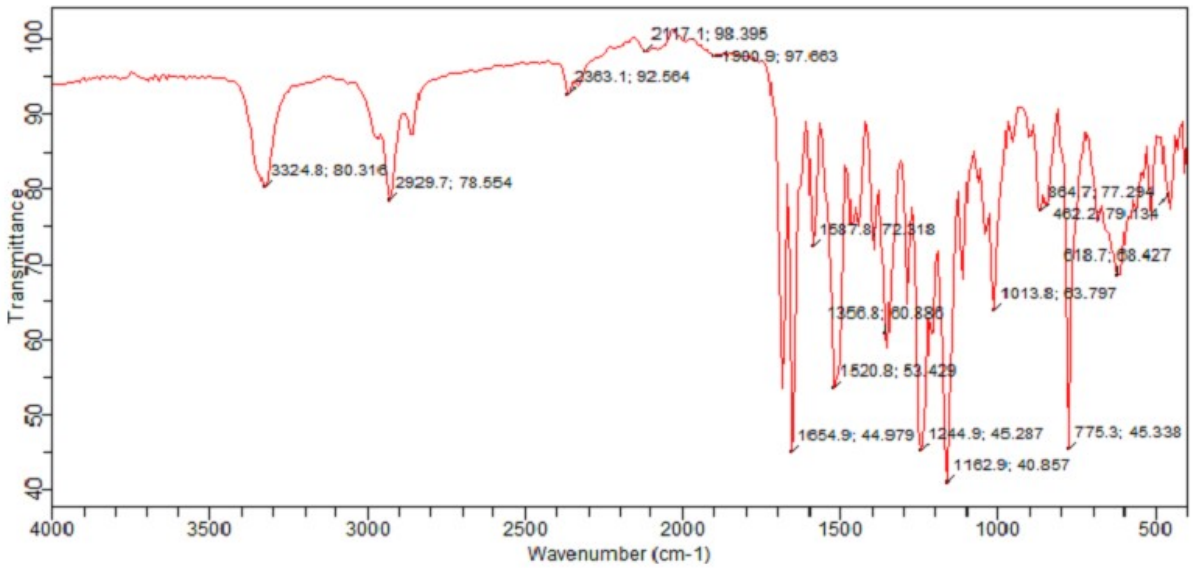

Figure 3c: FTIR Spectrum of compound **4.**

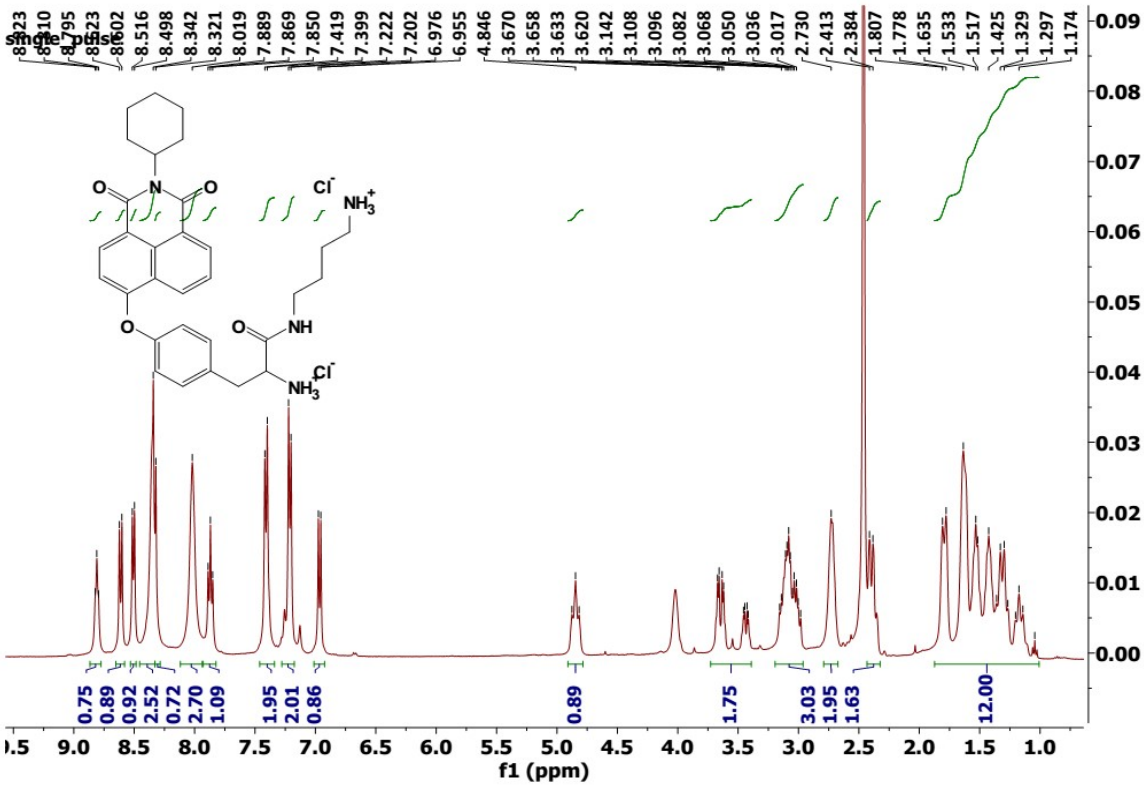

Figure 4a: ^{1}H NMR Spectrum of compound **YN-1.**

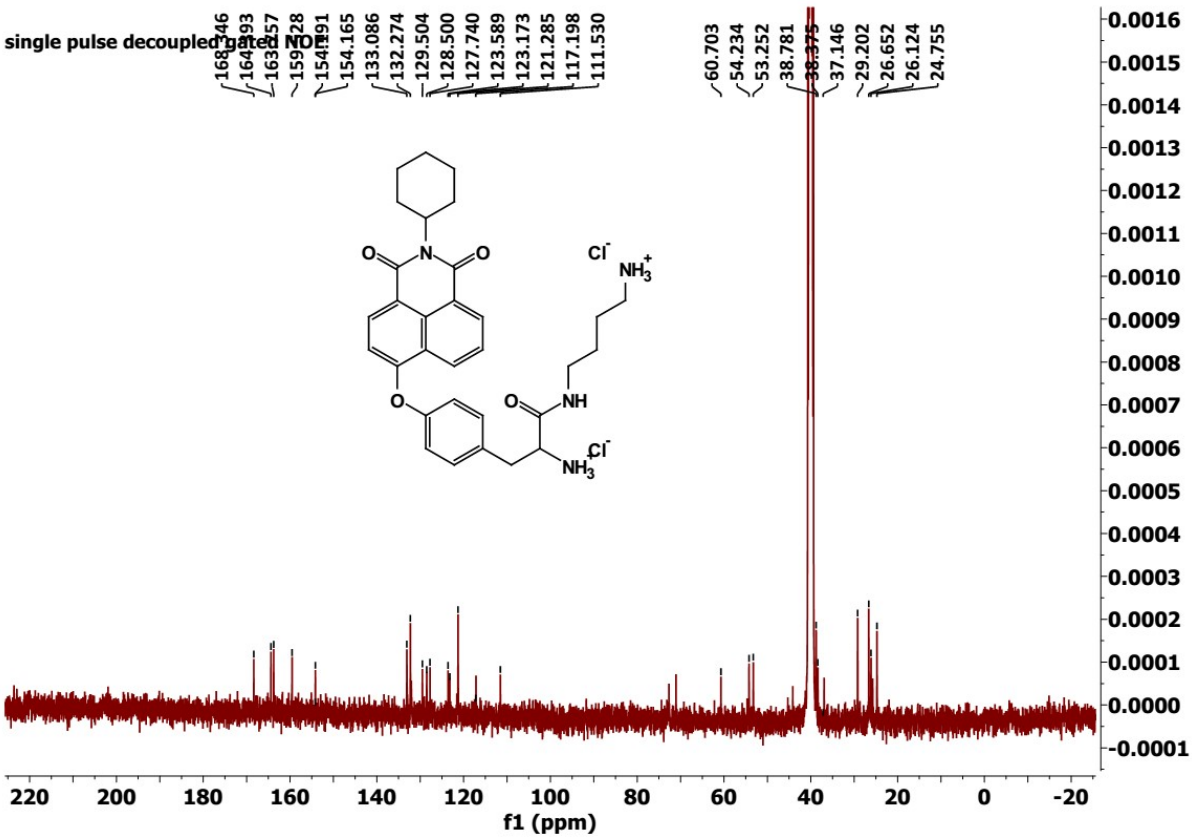

Figure 4b: ^{13}C NMR Spectrum of compound **YN-1.**

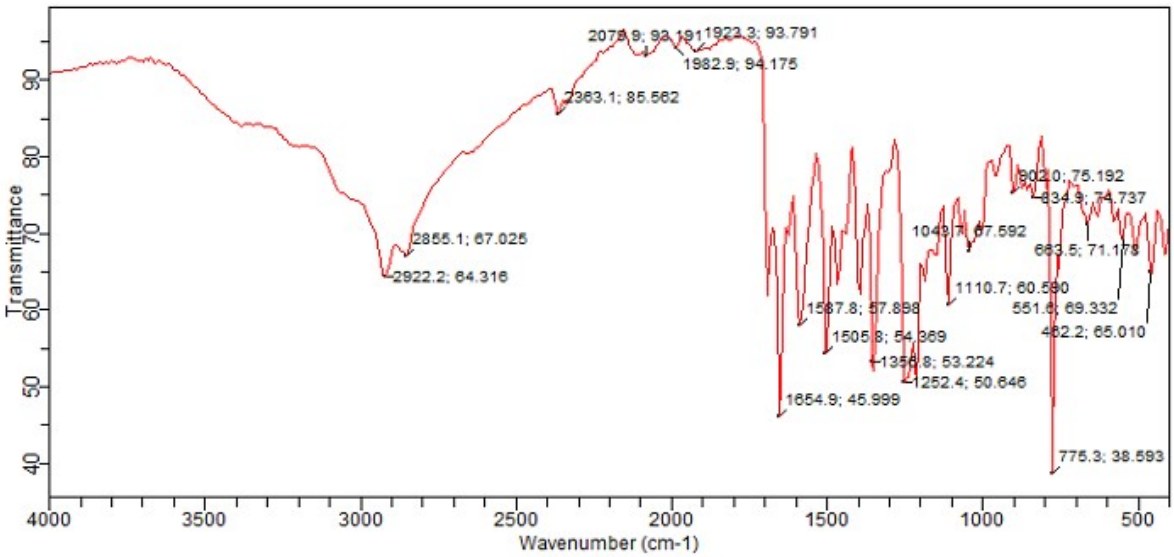

Figure 4c: FTIR Spectrum of compound **YN-1.**

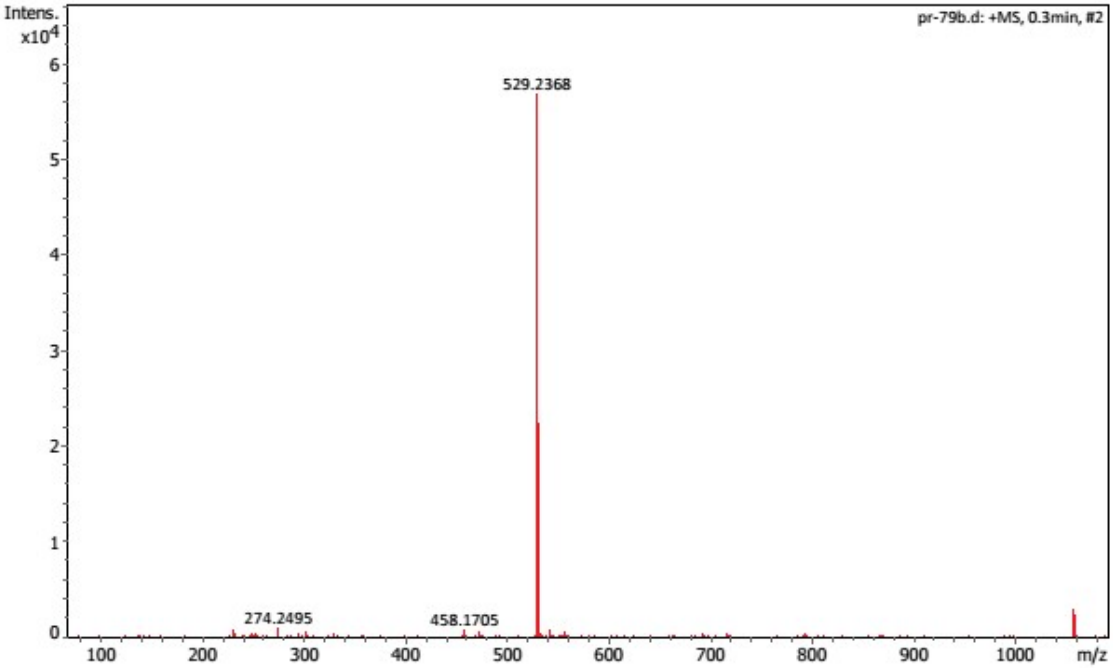

Figure 4d: Mass Spectrum of **YN-1**.

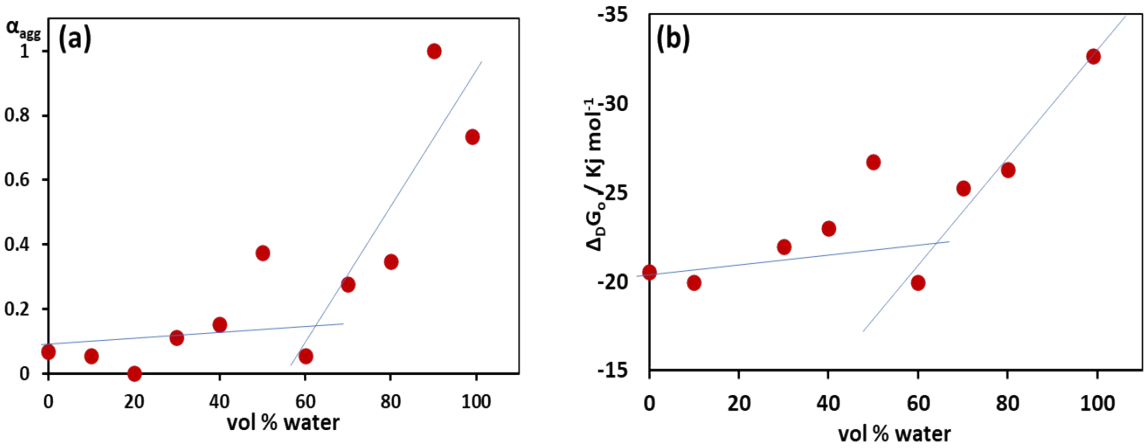

Figure S5: determination of degree of aggregation α_{agg} and Gibbs free energy (ΔG) from absorbance data recorded in 0–100 % water fraction in DMSO.

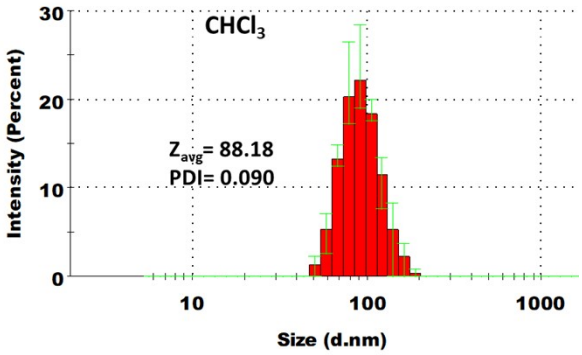

Figure S6a: Dynamic light scattering (DLS) data of YN-1 (5 μM) in $CHCl_3$.

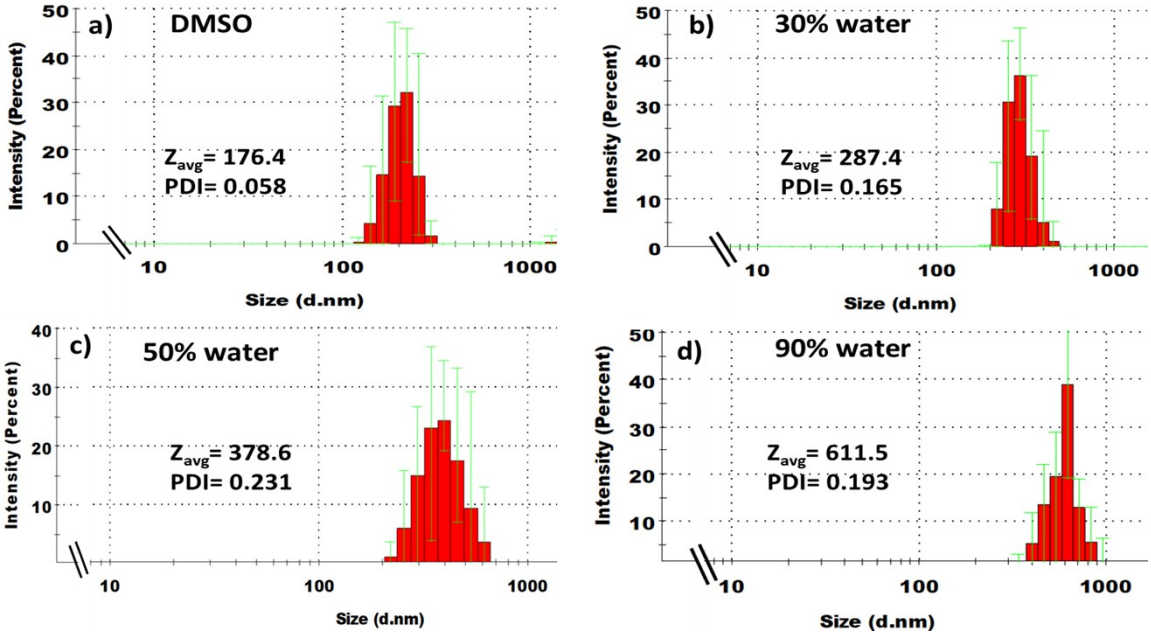

Figure S6b: Dynamic light scattering (DLS) data of **YN-1** (5 μM) in (a) DMSO and in different water fractions such as (b) 30% water; c) 50% water and; d) 90% water fractions in DMSO for measuring the size of aggregates.

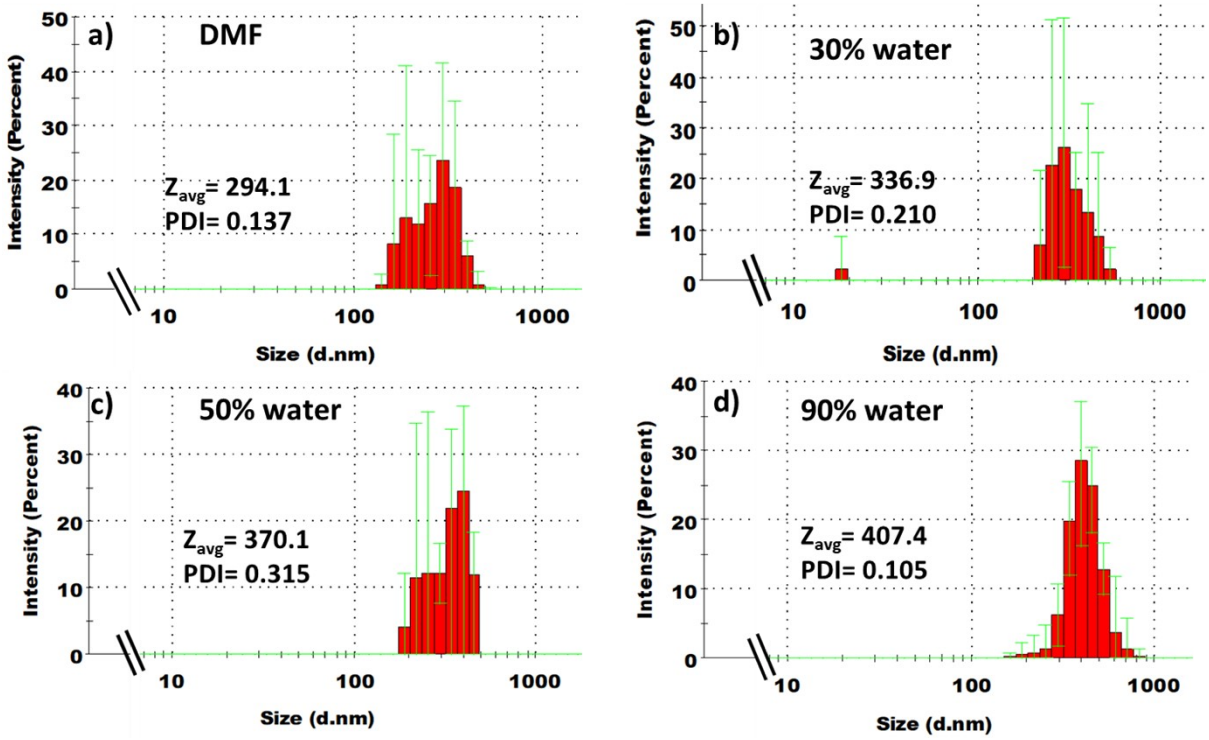

Figure S6c: Dynamic light scattering (DLS) data of **YN-1** (5 μM) in (a) DMF; and different water fractions such as (b) 30%; (c) 50% and (d) 90% in DMF for measuring the size of the aggregates.

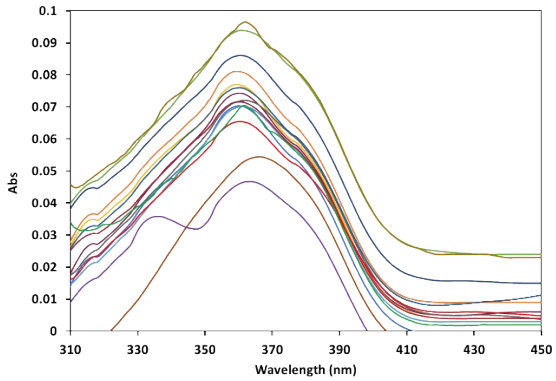

Figure S7: Absorbance spectrum of **YN-1** (10 μM) upon addition of NPPs in HEPES buffer: DMSO (2:8, v/v, pH 7.2) solution.

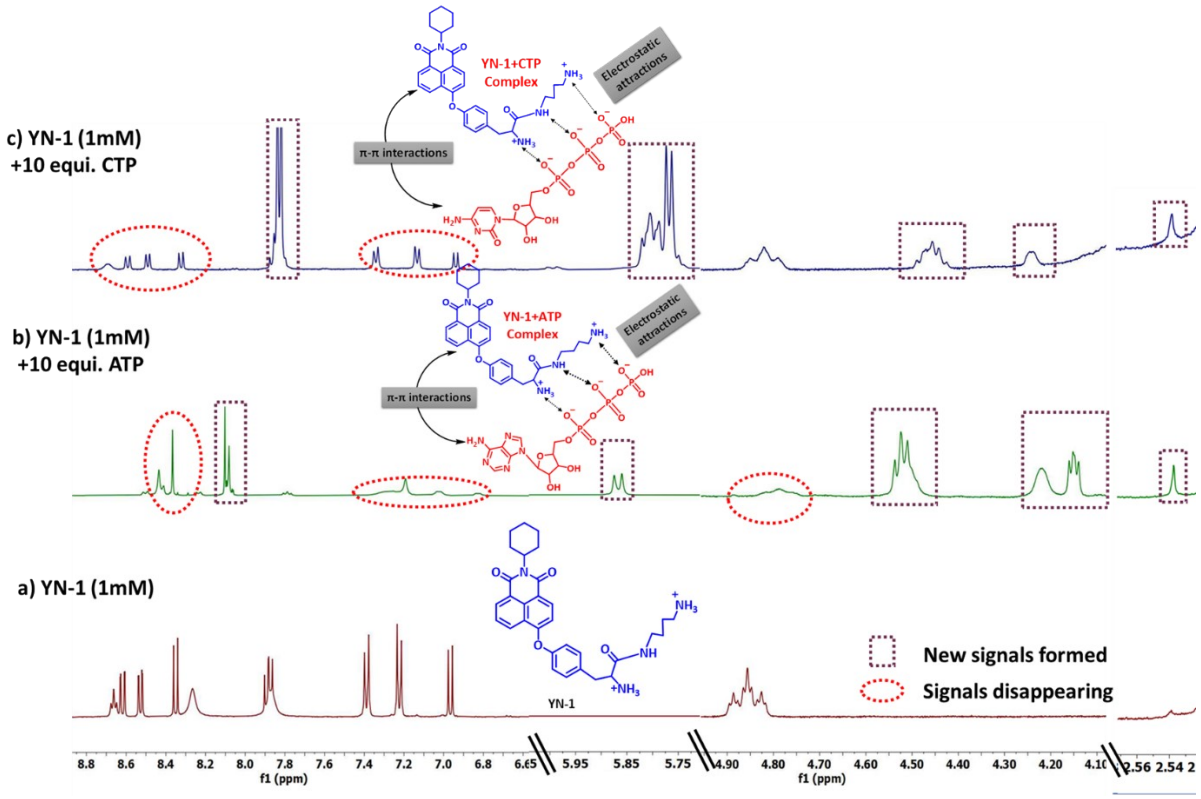

Figure S8: Partial ^{1}H NMR spectra of a) **YN-1** (1 mM) and upon addition of 10 equivalents of b) **YN-1**+ATP and; c) **YN-1**+CTP in DMSO-d_6 solvent showing proposed mechanism and comparison of concentration-based discrimination between ATP and CTP (10 equivalents).

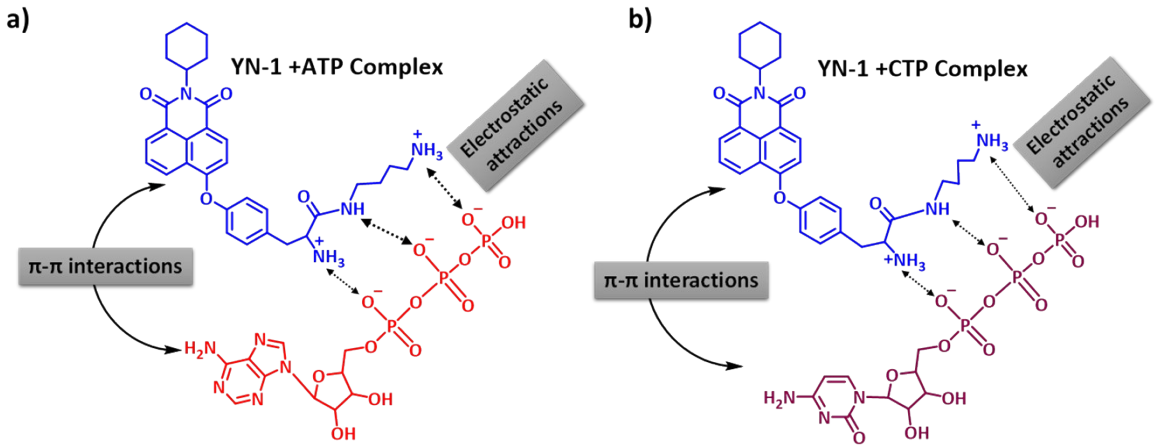

Figure S9: Proposed mechanism of a) **YN-1** (1 mM) +ATP; and b) **YN-1**+CTP.

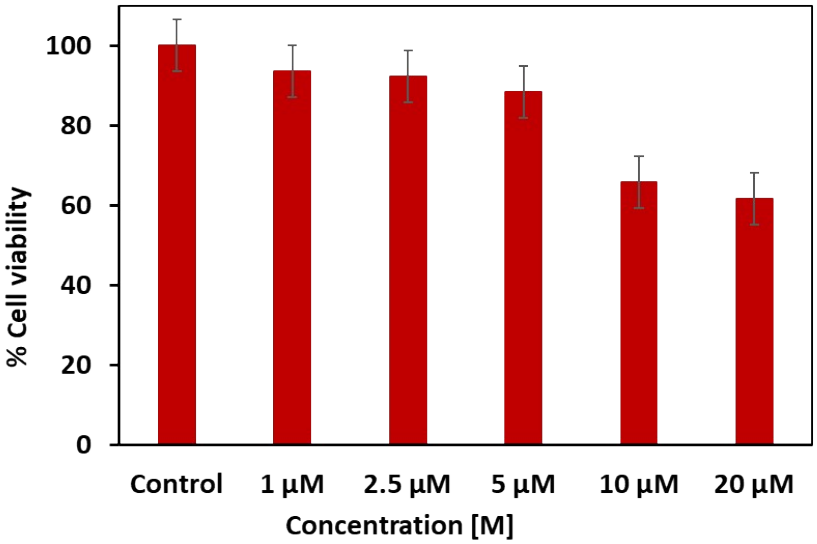

Figure S10. The MTT assay of **YN-1**.

Table S1. Summary of the reported fluorescent probes for ATP and CTP. HEPES: 4-(2-hydroxyethyl)-1-piperazineethanesulfonic acid; PBS: phosphate-buffered saline; Tris; tris(hydroxymethyl) aminomethane; DMSO: dimethyl sulfoxide; DMF: dimethylformamide; THF: tetrahydrofuran; λ_{ex}= excitation wavelenghth; λ_{em}= emission wavelength; Sensitivity: lowest detection limit.

Structure	Type	Selectivity	Media	Sensitivity	Applications	Ref.
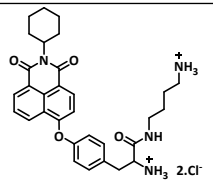 YN-1, Present Design	Turn-on (λ_{ex}= 360 nm, λ_{em}= 440 nm)	ATP and CTP	HEPES buffer: DMSO (2:8, v/v, pH 7.2)	1.72 nM (ATP); 7.1 nM (CTP)	Cell imaging	Present Manuscript
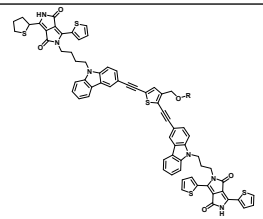	Turn-on (λ_{ex}= 323 nm, λ_{em}= 550 nm)	ATP	THF: H_2O (1:1, v/v)	19.6 μM	-	1.
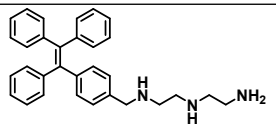	Turn-on (λ_{ex}= 315 nm, λ_{em}= 564 nm)	ATP	PBS buffer (pH = 7.4)	5 μM	Cell imaging	2.
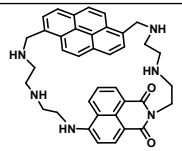	Turn-on (λ_{ex}= 350 nm, λ_{em}= 380 nm and 550 nm)	ATP CTP	DMSO: TRIS buffer+100 mM NaCl (0.2:9.8, *v/v*, pH = 7.4)	0.08 mM	-	3.

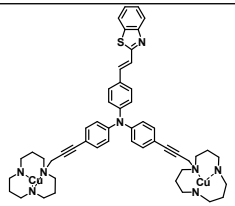	Turn-on (λ_{ex}= 405 nm, λ_{em}= 560 nm)	ATP	H_2O	0.43 μM	Cell imaging	4.
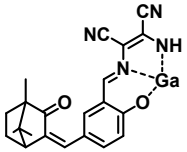	Turn-on (λ_{ex}= 425 nm, λ_{em}= 602 nm)		DMF: PBS buffer (0.1:9.9, *v/v*, pH = 7.4)	67.4 nM	Cell imaging	5.
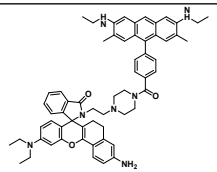	Turn-on (λ_{ex}= 500 nm, λ_{em}= 560 nm)	ATP	HEPES (pH 7.4+10% C_2H_5OH)	3 mM	Cell imaging	6.
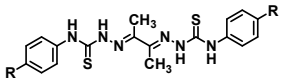	Turn-on (λ_{ex}= 500 nm, λ_{em}= 560 nm)	Zn^{2+} and ATP	CH_3CN: 0.01 M HEPES (9:1, *v/v*; pH 7.4)	6.7 μM (for 1) and 1.7 μM (for 2)	-	7.
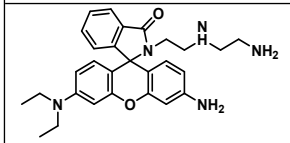	Turn-on (λ_{ex}= 480 nm, λ_{em}= 634 nm)	ATP	C_2H_5OH:H_2O: PBS (0.1:9.9, *v/v*)	0.05 μM	Cell imaging	8.
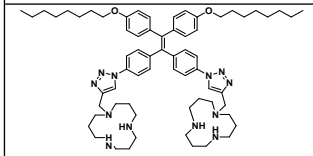	Turn-on (λ_{ex}= 345 nm, λ_{em}= 471 nm)	ATP	H_2O	1.5 μM	Cell imaging	9.

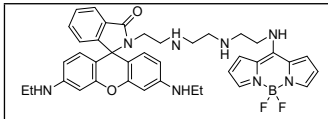	Turn-on (λ_{ex}= 403 nm, λ_{em}= 557 nm)	ATP	HEPES buffer (pH 5.5)	-	-	10.
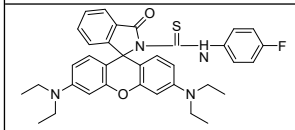	Turn-on (λ_{ex}= 510 nm, λ_{emi}= 591 nm)	ATP ADP CTP	DMSO: PBS (4:6, *v/v*)	-	Cell imaging	11.
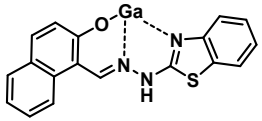	Turn-off (λ_{ex}= 440 nm, λ_{em}= 518 nm)	ATP ADP	DMSO:water (9:1, *v/v*)	-	Cell imaging and In vivo images of zebrafish.	12.
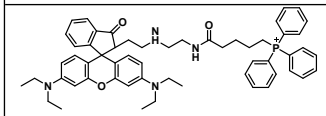	Turn-on (λ_{ex}= 520 nm, λ_{em}= 583 nm)	ATP	PBS buffer (pH 7.4)	0.033 mM	Cell imaging	13.
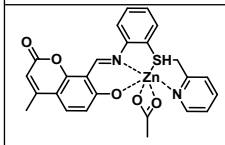	Turn-off (λ_{exc}= 315 nm, λ_{emi}= 512 nm)	ATP	CH_3OH:water (3:1, *v/v*)	6.6 μM	Cell imaging	14.
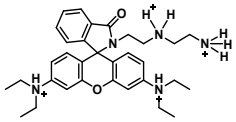	Turn-on (λ_{ex}= 510 nm, λ_{em}= 583 nm)	ATP	HEPES buffer (pH 7.2)	-	Cell imaging	15.

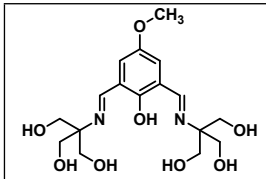	Turn-off (λ_{ex}= 457 nm, λ_{em}= 560 nm)	ATP and CTP	TRIS HCl buffer (pH 7.2)	3.9 µM (ATP) and 8.3 µM (CTP)	-	16.
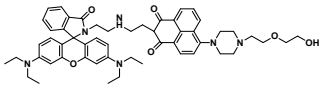	Turn-on (λ_{ex}= 420 nm, λ_{em}= 580 nm)	ATP	HEPES (pH = 7.2)	0.1 µM	Cell imaging	17.
Terbium(III)-organic framework	Turn-off (λ_{ex}= 330 nm, λ_{emi}= 493 nm,546 nm, 586 nm and 623 nm)	CTP	DMF:water (1 : 1, v/v)	-	-	18.
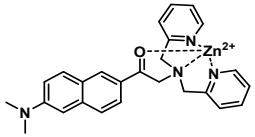	Turn-on (λ_{exc}= 370 nm, λ_{emi}= 538 nm)	ATP ADP	HEPES buffer (pH 7.4, 1% MeCN)	1.0 µM	Cell imaging	19.
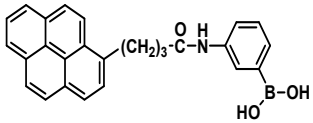	Turn-on (λ_{ex}= 342 nm, λ_{em}= 482 nm)	ATP	Polycation buffer (pH 10.2, 0.5 mM Na_2CO_3, 0.5 mM $NaHCO_3$)	0.1 µM	In vitro	20.

References

1. D. Giri, S. K. Raut, C. K. Behera, S. K. Patra, , Diketopyrrollopyrrole anchored carbazole-alt-thiophene based Fe^{3+}-coordinated metallopolymer for the selective recognition of ATP, *Polymer*, 2022, **253**, 124951.
2. N. H. Kim, B. W. Kim, H. Moon, H. Yoo, R. H. Kang, J. K. Hur, Y. Oh, B. M. Kim, D. Kim, AIEgen-based nanoprobe for the ATP sensing and imaging in cancer cells and embryonic stem cells, *Analytica Chimica Acta*, 2021, **1152**, 338269.
3. A.M. Agafontsev, A.S. Oshchepkov, T.A. Shumilova, E.A. Kataev, Binding and Sensing Properties of a Hybrid Naphthalimide–Pyrene Aza-Cyclophane towards Nucleotides in an Aqueous Solution, *Molecules*, 2021, **26**, 980.
4. W. Sun, G. Liu, M. Tong, H. Wang, S. Liu, A mitochondria-targeting fluorescent sensor for on–off–on response to Cu^{2+} and ATP in cells and zebrafish, *Analyst*, 2021, **146**, 1892–1896.
5. Z. Wang, Y. Zhang, J. Yin, M. Li, H. Luo, Y. Yang, X. Xu, Q. Yong, S. Wang, An easily available camphor-derived ratiometric fluorescent probe with AIE feature for sequential Ga^{3+} and ATP sensing in a near-perfect aqueous media and its bio-imaging in living cells and mice, *Sensors & Actuators: B. Chemical*, 2020, **320**, 128249.
6. T.-B. Ren, S.-Y. Wen, L. Wang, P. Lu, B. Xiong, L. Yuan, X.-B. Zhang, Engineering a reversible fluorescent probe for real-time live-cell imaging and quantification of mitochondrial ATP, *Analytical Chemistry*, 2020, **92**, 4681-4688.
7. P. Adak, B. Ghosh, A. Bauza, A. Frontera, S. R. Herron, S. K. Chattopadhyay, Binuclear and tetranuclear Zn(II) complexes with thiosemicarbazones: synthesis, X-ray crystal structures, ATP-sensing, DNA-binding,phosphatase activity and theoretical calculations, *RSC Advances*, 2020, **10**, 12735-12746.
8. A.F. Tikum, G. Kim, A. Nasirian, J.W. Ko, J. Yoon, J. Kim, Rhodamine-based near-infrared probe for emission detection of ATP in lysosomes in living cells, *Sensors and Actuators B: Chemical*, 2019, **292**, 40-47.
9. A.-X. Ding, Y.-D. Shi, K.-X. Zhang, W. Sun, Z.-L. Tan, Z.-L. Lu, L. He, Self-assembled aggregation-induced emission micelle (AIE micelle) as an interfacial fluorescence probe for sequential recognition of Cu^{2+} and ATP in water, *Sensors and Actuators B: Chemical*, 2018, **255**, 440-447.
10. Y.W. Jun, T. Wang, S. Hwang, D. Kim, D. Ma, K.H. Kim, S. Kim, J. Jung, K.H. Ahn, A Ratiometric Two-Photon Fluorescent Probe for Tracking Lysosomal ATP: Direct In Cellulo Observation of Lysosomal Membrane Fusion Processes, *Angewandte Chemie*, 2018, **130**, 10299-10304.
11. Y. Liu, D. Lee, D. Wu, K. Swamy, J. Yoon, A new kind of rhodamine-based fluorescence turn-on probe for monitoring ATP in mitochondria, *Sensors and Actuators B: Chemical*, 2018, **265**, 429-434.
12. X. Zhang, Y. Jiang, N. Xiao, Monitoring ADP and ATP in vivo using a fluorescent Ga (III)-probe complex, *Chemical Communications*, 2018, **54**, 12812-12815.
13. K.-Y. Tan, C.-Y. Li, Y.-F. Li, J. Fei, B. Yang, Y.-J. Fu, F. Li, Real-time monitoring ATP in mitochondrion of living cells: a specific fluorescent probe for ATP by dual recognition sites, *Analytical chemistry*, 2017, **89**, 1749-1756.
14. C. Patra, C. Sen, A.D. Mahapatra, D. Chattopadhyay, A. Mahapatra, C. Sinha, Pyridylthioether-hydroxycoumarin Schiff base as selective Zn^{2+} fluorescence sensor, application in life cell imaging and uses of resulting complex as a secondary probe for ATP sensing, *Journal of Photochemistry and Photobiology A: Chemistry*, 2017, **341**, 97-107.
15. D. de la Fuente-Herreruela, V. Gónzalez-Charro, V.G. Almendro-Vedia, M. Morán, M.Á. Martín, M.P. Lillo, P. Natale, I. López-Montero, Rhodamine-based sensor for real-time imaging of

mitochondrial ATP in living fibroblasts, *Biochimica et Biophysica Acta (BBA)-Bioenergetics*, 2017, **1858**, 999-1006.

16. A. K. Gupta, A. Dhir, C. P. Pradeep, Ratiometric Detection of Adenosine-5'-triphosphate (ATP) and Cytidine-5'-triphosphate (CTP) with a Fluorescent Spider-Like Receptor in Water, *Eur. J. Org. Chem.*, 2015, **1**, 122–129.
17. L. Tang, C.-Y. Li, Y.-F. Li, C.-X. Zou, A ratiometric fluorescent probe with unexpected high selectivity for ATP and its application in cell imaging, *Chemical Communications*, 2014, **50**, 15411-15414.
18. Xi Juan Zhao, Rong Xing He, Yuan Fang Li, A terbium(III)-organic framework for highly selective sensing of cytidine triphosphate, *Analyst*, 2012, **137**, 5190–5192.
19. A.S. Rao, D. Kim, H. Nam, H. Jo, K.H. Kim, C. Ban, K.H. Ahn, A turn-on two-photon fluorescent probe for ATP and ADP, *Chemical Communications*, 2012, **48**, 3206-3208.
20. Y. Kanekiyo, R. Naganawa, H. Tao, Fluorescence detection of ATP based on the ATP-mediated aggregation of pyrene-appended boronic acid on a polycation, *Chemical communications*, 2004, 1006-1007.